The ultrasonic wave interaction with porosity defects in welded rail head

E. Jasiūnienė, E. Žukauskas

Ultrasound Institute, Kaunas University of Technology,
Studentu 50, LT-51368 Kaunas, Lithuania

Abstract

There are several millions aluminothermic welds and thousands of new welds being made daily on the European rail network. Although the aluminothermic welding technique is well proven, it is a critical safety component of the rail infrastructure. The consequences of a single failure could result in the derailment.

The objective of this investigation was to verify the influence of the depth of the porosity type defect on strength of the reflected ultrasonic signal when the ultrasonic phased array is at the fixed position. The propagation of the ultrasonic wave in the rail head with porosity type defects has been modelled using ANSYS finite element code and CIVA software.

The presented results demonstrate the influence of the depth of the porosity defect for 35 mm weld, when the defect is located in the middle of the weld.

Keywords: rail, weld, porosity, ultrasonic NDT, phased array, finite element modelling, CIVA

Introduction

There are several millions aluminothermic welds and thousands of new welds being made daily on the European rail network. Although the aluminothermic welding technique is well proven, it is a critical safety component of the rail infrastructure. An increase in rail speeds, density of rail traffic and train weights are now causing an increasing number of rail breaks across the European rail network. The consequences of a single failure could result in the derailment [1].

The vast majority of ultrasonic inspection of rail welds is performed by operators using handheld conventional angle beam transducers, which are manually scanned. Generally for welded objects with thicknesses under about 20 mm a 60° and 70° probes are used, and for thicknesses over 20 mm, 45° and 60° probe angles are recommended [2]. The refraction angles generally used for testing of rail welds are 45° and 70° degrees [3]. In European and British standards [4] for railway applications for a test of the head zone of the weld, non-planar defects, 2MHz transducer with 70° angle (shear waves) (Fig. 1) is recommended.

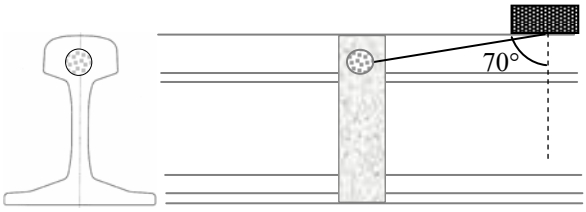

Fig. 1. **Positioning of the probes for testing the weld of a rail head according to European and British standards [4]**

In order to test the whole volume of a weld without mechanical scanning, ultrasonic arrays should be used. Advantages of using phased arrays are: possibility to focus the beam by applying electronic time delay laws and to use the linear and sectorial electronic scanning [5-7]. Main advantage of the ultrasonic arrays is that one array can be used to perform a number of different inspections [8].

The main type of the defect in the head of the rail, which has to be found, is porosity. Gas porosity results from the entrapment of discrete gas pockets within solidifying metal and can weaken the weld microstructure [9]. It was determined that porosity is most damaging at a depth of 15 mm below the running surface of the rail [10].

The objective of this investigation was to verify the influence of the depth of the porosity type defect on a strength of the reflected ultrasonic signal when the ultrasonic phased array is at the fixed position. The propagation of the ultrasonic wave in a rail head with porosity type defect (Fig.2) has been modelled using ANSYS finite element code and CIVA software.

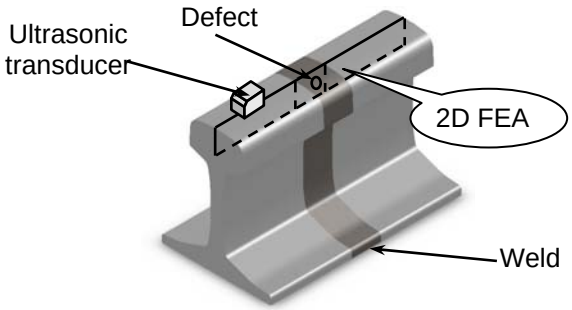

Fig.2 **Part of the rail under investigation**

Modelling using CIVA software

Modelling of beam-defect interaction using the CIVA software applies approximated theories such as Kirchhoff approximation. The software inputs are the geometry and the acoustic properties of the rail material.

The components requiring defect response predictions need to be imported as two-dimensional DXF or CAD files or drawn in two-dimensional profile in CAD environment included in the CIVA software. After the two-dimensional profile is created or imported, it can be subsequently extruded to create the three-dimensional solid model. Three-dimensional solid models can be imported into the CIVA, but currently only for ultrasonic field predictions. So, the 2D rail profile was drawn in the CIVA CAD environment using the given parameters and extruded subsequently to form the 3D rail profile.

During the modelling it was assumed that the test object material is steel. Velocities of longitudinal and shear ultrasonic waves in the test object were obtained experimentally. The velocity of a longitudinal wave is 5840 m/s and the velocity of a shear wave is 3290 m/s. The density of the test object is 7800 kg/m^3. The defects were modelled as air-spheres with the 5 mm diameter, in the middle of the 35 mm weld with different distances from the top surface of the rail - 5 mm, 7.5 mm, 10 mm and 12.5 mm.

For modelling 32 elements 2MHz linear phased array was used. Array parameters were the following: the width of the element is 0.67 mm, the gap between elements is 0.08 mm, the pitch is 0.75 mm, the active aperture is 23.92 mm and the passive aperture is 10 mm. The transducer was excited using 2 MHz signal shown in Fig. 3, the sampling frequency was 40 MHz, the bandwidth 65%. The phased array was used in a sectorial scanning mode; the beam was scanned from 30° to 70° degrees with a step of one degree.

Positioning of the probe on the sample and position of defects in the sample is shown in Fig. 4. The length of the rail sample used in the modelling was 300 mm. The zoomed image of the inspected zone with positions of porosity type defects is shown in Fig.5.

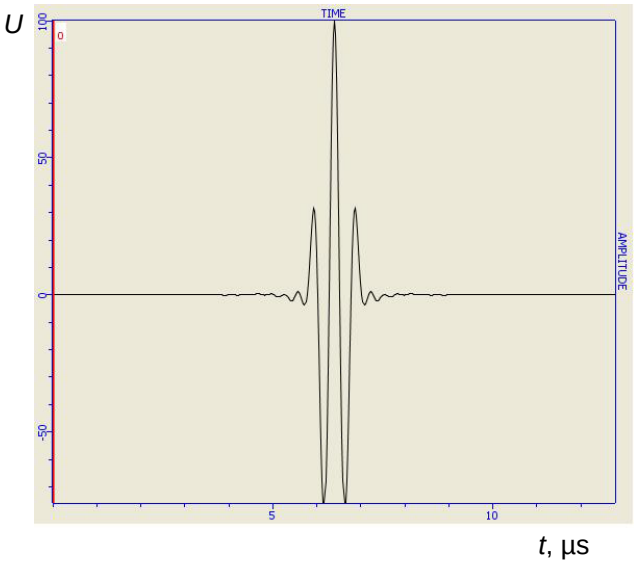

Fig. 3. **Waveform of the excitation signal**

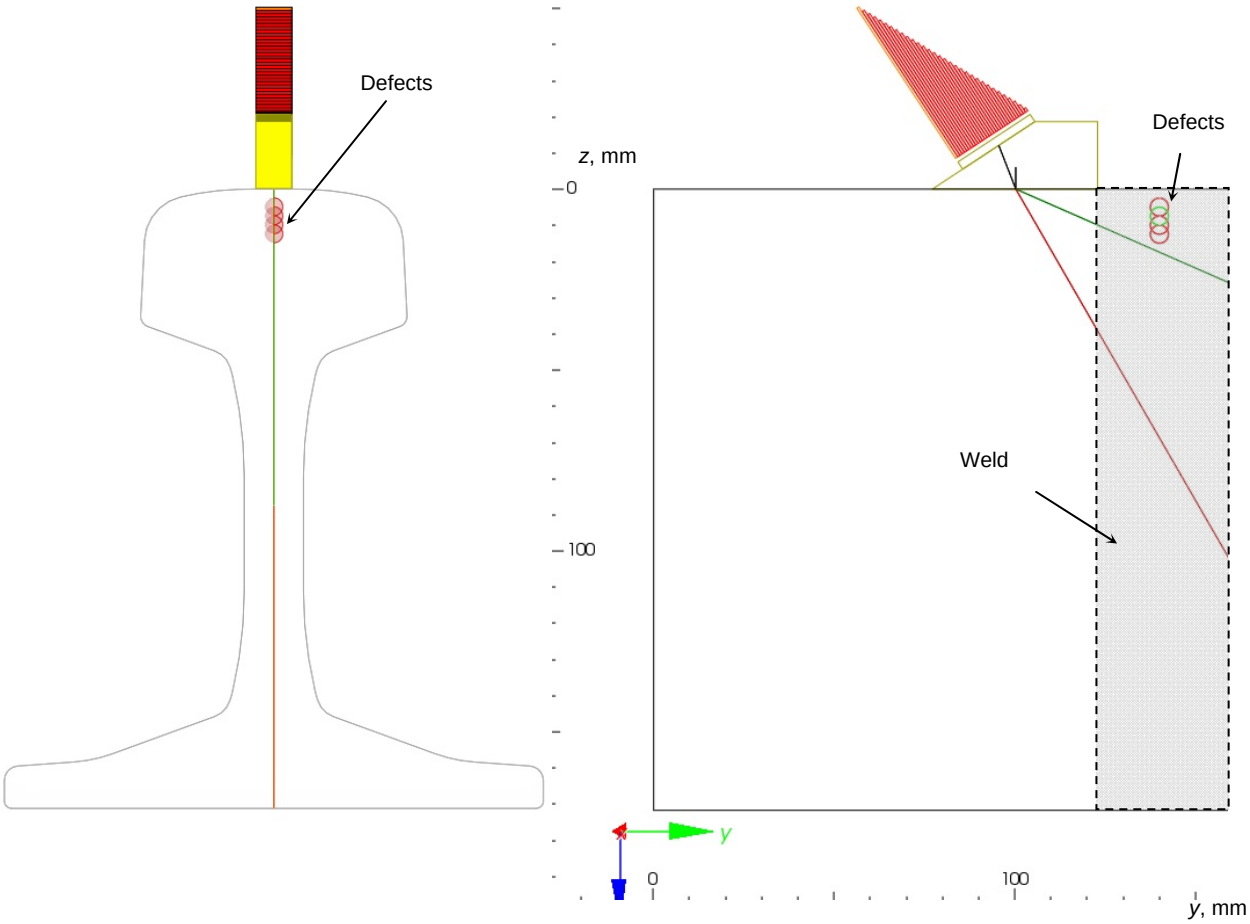

Fig. 4. **Positioning of the transducer array on the sample and position of the porosity type defects in the sample**

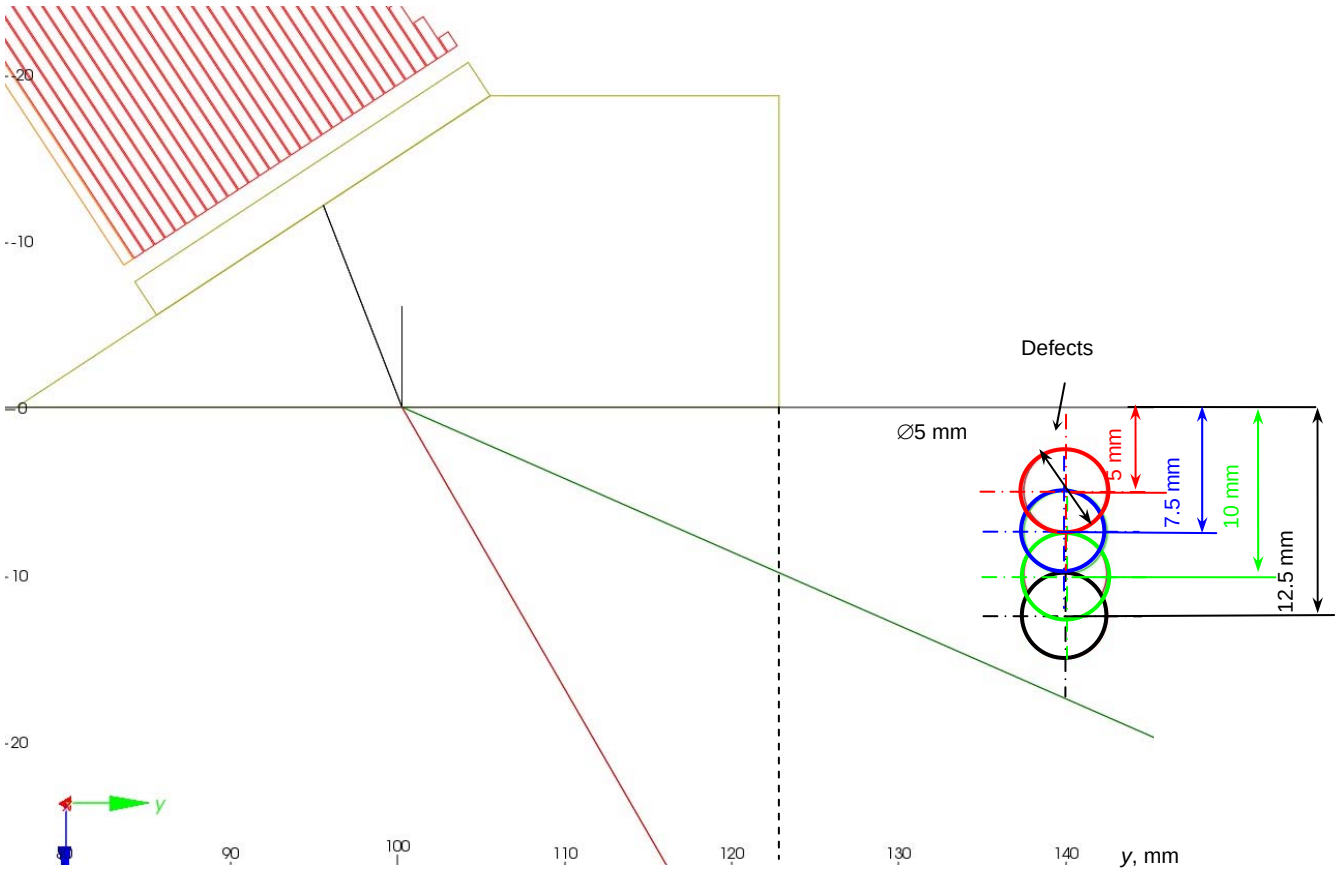

Fig. 5**. Zoomed image of the inspected zone**

2D finite element modelling

In the ANSYS finite element code to solve the transient wave equation implicit algorithm was used. Because modelling of the 3D object using finite elements requires huge computer resources and time, the case was simplified using 2D approach. Graphical representation of the 2D model is presented in Fig.6.

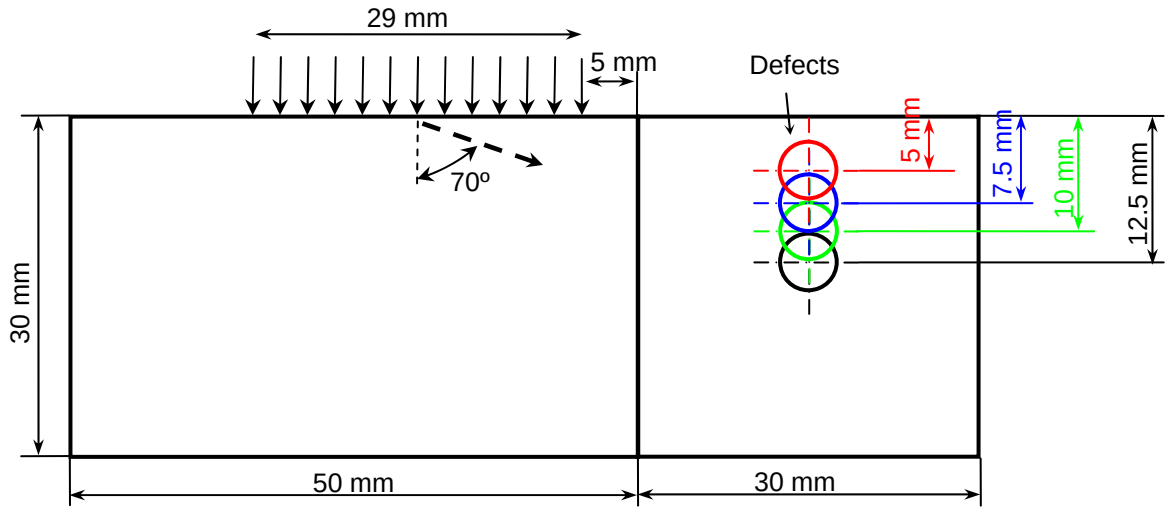

Fig.6.**Graphical representation of the 2D model of the welded rail head with porosity type defects at different depths**

Area of the model was meshed using PLANE42 elements, which are used for modelling of the solids. The element is defined by four nodes having two degrees of freedom at each node. The spatial resolution of the mesh is 0.1 mm and corresponds to 1/15 of the wavelength. The excitation frequency of the ultrasonic wave is 2 MHz and the size of integration step in the time domain is 25 ns. The weld and rail interface in the finite element model was modelled ideally connecting nodes on contacting edges of steel and weld areas.

Elastic properties of steel and weld were calculated using measured values of velocities of longitudinal and shear ultrasonic wave and are presented in Table 1:

Table 1. **Elastic properties of materials used in FE modelling**

	Young's modulus, GPa	Poisson's ratio
Steel	212.8	0.287
Weld	214	0.267

The excitation of the ultrasonic wave was modelled by a transient force applied on a surface of the material in a contact zone between the ultrasonic transducer and material under investigation. It was assumed that due to the coupling liquid only vertical component of displacement of the transducer is transmitted through the contact surface. So, the direction of the excitation force is normal to the surface of the material. The waveform of the transient force used in finite element modelling is presented in Fig.7.

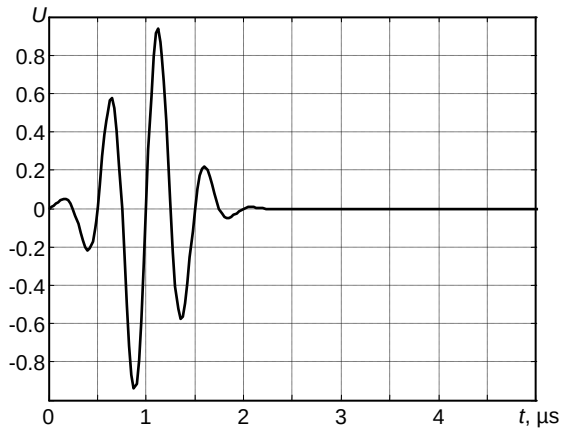

Fig.7. **Time diagram of the force applied on the surface of the material**

The required angle of the ultrasonic wave propagation in a test material is obtained by the time delay of the excitation signals applied at the different nodes in the excitation zone. The delay time of forces at different nodes depends on a distance between nodes and the velocity of the wave of interest. The propagation angle of the ultrasonic wave was calculated for a shear wave and the propagation angle of 70º.

Modelling results

At first, the numerical modelling was carried out when the depth of the defect is 12.5 mm from the surface of the rail head. In this case the ultrasonic wave propagates direct to the defect with 70º degree angle. The defect response, modelled using the CIVA software is presented in Fig. 8. The time diagram of the signal reflected from the defect modelled using the ANSYS finite element code is presented in Fig.9. This signal will be used as a reference for normalization of the other signals (from the defects at different depths). Snapshots of the velocity modulus fields at different instances of the time are presented in Fig.10. When the transient force is applied on the nodes, the shear and surface waves are generated. When the shear wave reaches the defect, reflection occurs and the reflected wave travels back to the excitation zone. Signals were registered on the nodes, which were used for excitation of the ultrasonic wave, i.e. at the position of the virtual ultrasonic transducer and phased in reverse order.

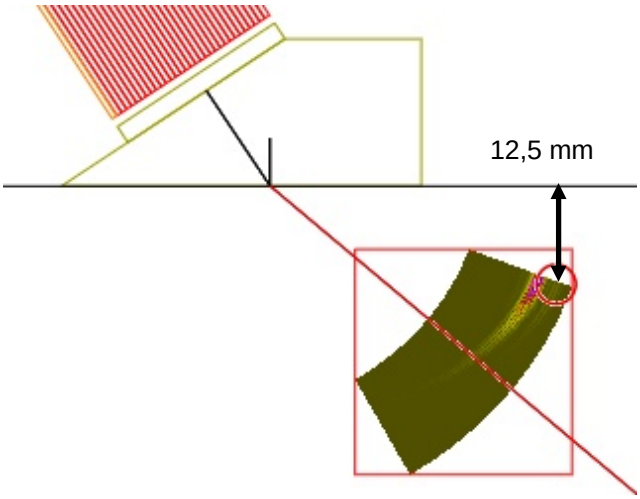

Fig.8. **Defect response from the defect at 12.5 mm depth**

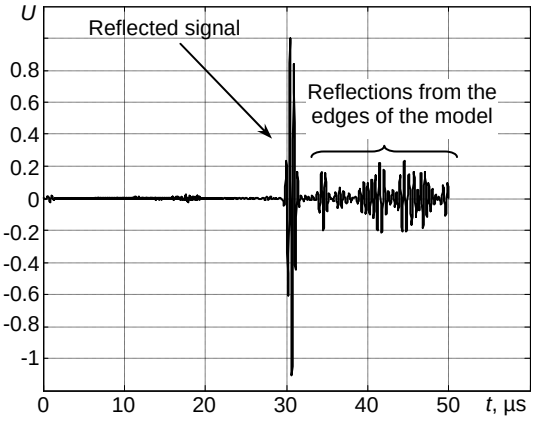

Fig.9. **Normalized time diagram of the signal reflected from the defect at 12.5 mm depth**

The defect response in the case when a porosity defect is located at 10 mm from the surface of the rail, modelled using the CIVA software is presented in Fig. 11. The time diagram of the signal reflected from the defect modelled using the ANSYS finite element code for the same case is presented in Fig.12. When the depth of the defect is 10 mm, the amplitude of the reflected signal is 60% of the reference signal.

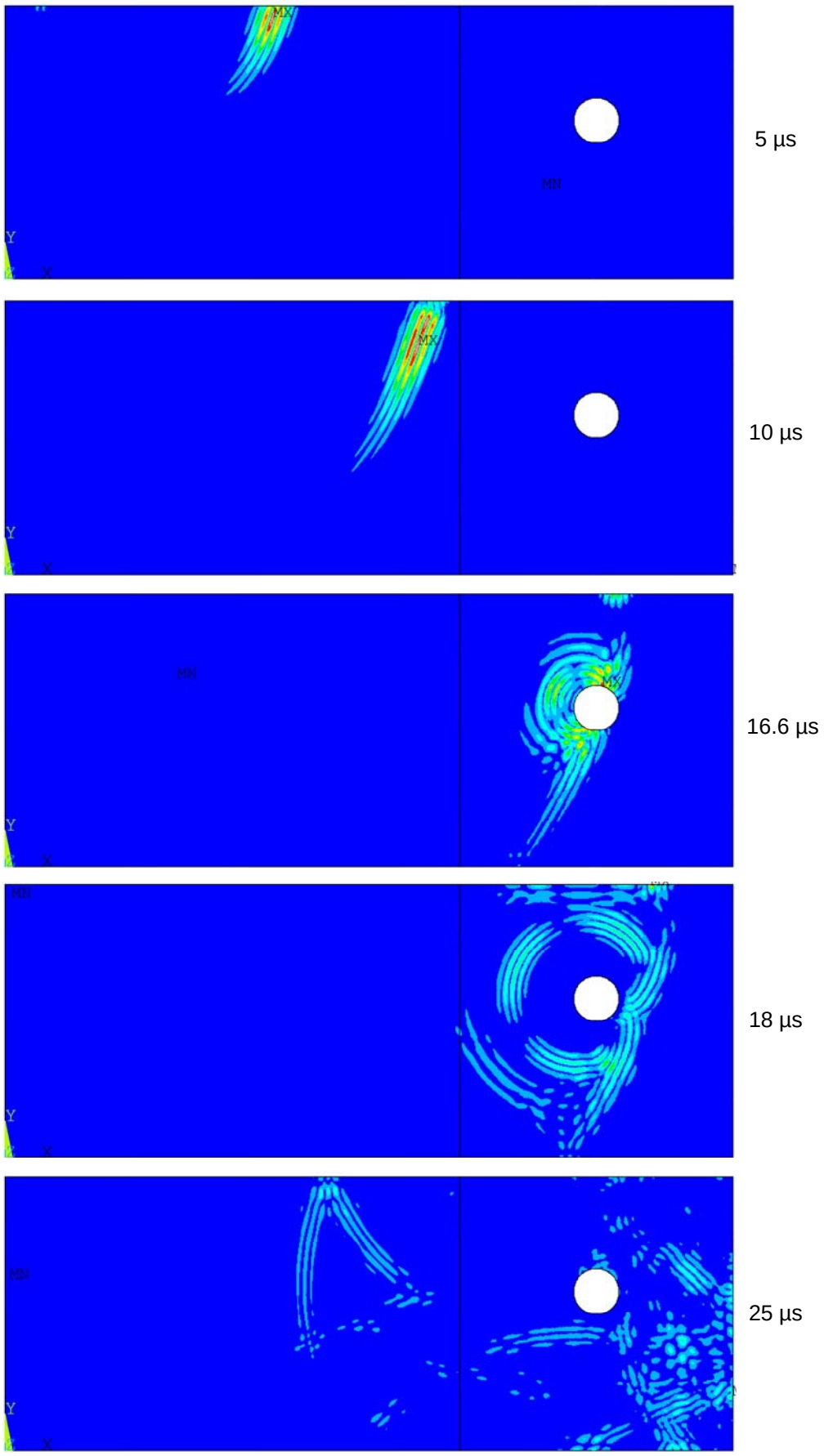

Fig.10. **The snapshots of the particle velocity modulus field at different instances of time in the case when the defect is located at 12.5mm from the surface of the rail**

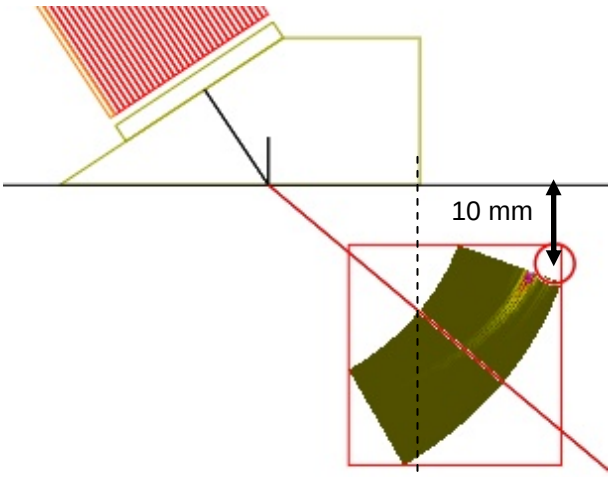

Fig.11. **Defect response from the defect at 10 mm depth**

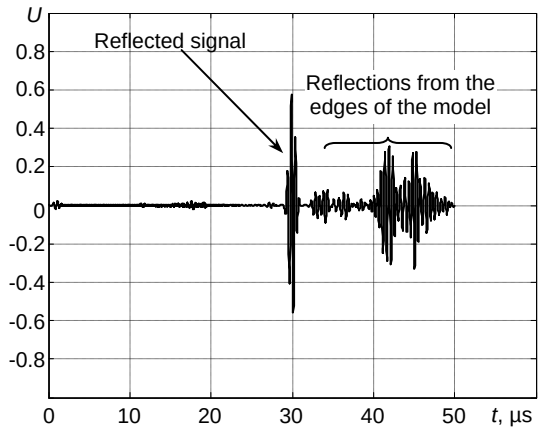

Fig.12. **Normalized time diagram of the signal reflected from the defect at 10 mm depth**

The defect response in the case when the porosity defect is located at 7.5 mm from the surface of the rail, modelled using the CIVA software is presented in Fig. 13. The time diagram of the signal reflected from the defect modelled using the ANSYS finite element code for the same case is presented in Fig.14. When the depth of the defect is 7.5 mm. the amplitude of the reflected signal is 20% of the reference signal.

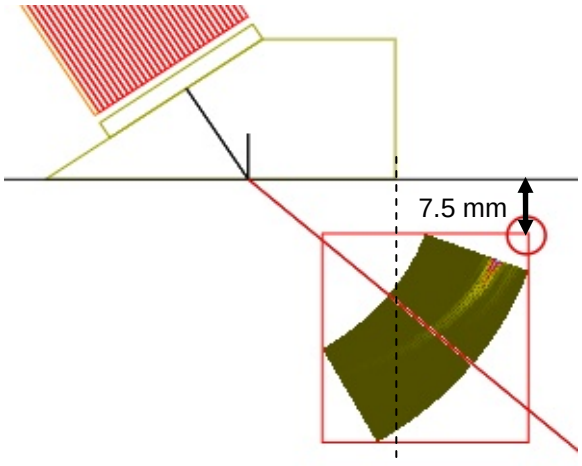

Fig.13. **Defect response from the defect at 7.5 mm depth**

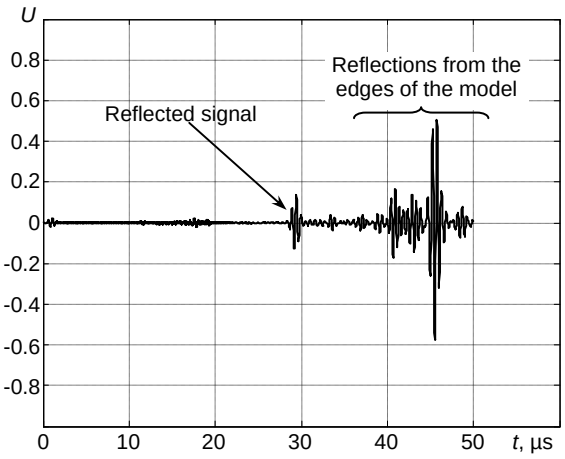

Fig.14. **Normalized time diagram of the signal reflected from the defect at 7.5 mm depth**

The defect response in the case when the porosity defect is located at 5 mm from the surface of the rail, modelled using the CIVA software is presented in Fig. 15. The time diagram of the signal reflected from the defect modelled using the ANSYS finite element code for the same case is presented in Fig.16. When the depth of the defect is 5 mm, the amplitude of the reflected signal is only 2% of the reference signal.

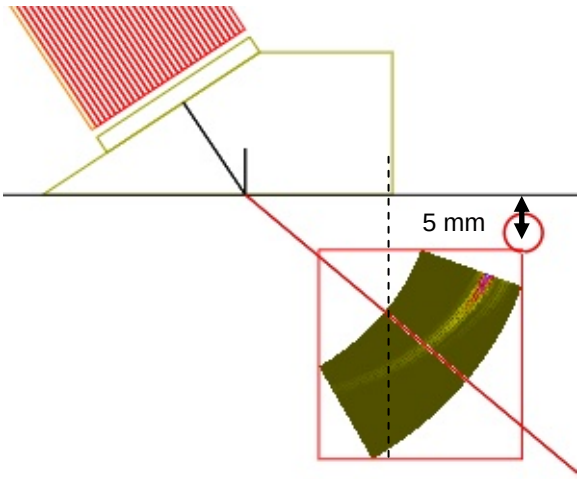

Fig.15. **Defect response from the defect at 5 mm depth**

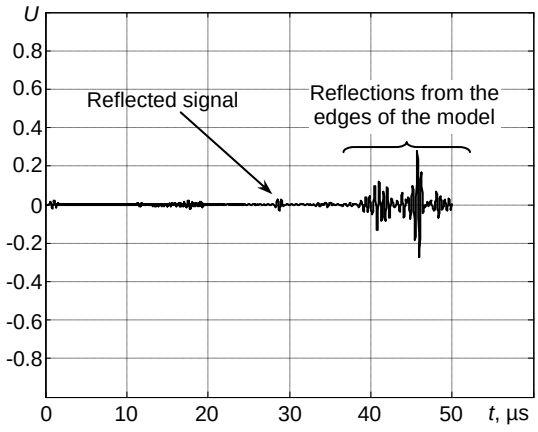

Fig.16. **Normalized time diagram of the signal reflected from the defect at 5 mm depth**

Dependence of the amplitude of the reflected signals on the depth of the defects is presented in Fig.17 (linear scale) and Fig.18 (logarithmic scale). From the presented results it can be seen, that the detectibility of the defects decreses drastically, when the distance of the defect from the top surface of the rail is larger than 10mm and if the ultrasonic transducer array is positioned beside the weld.

Fig.17. **Dependence of the amplitude of the reflected signals from the distance of the defect from the top surface of the rail (linear scale)**

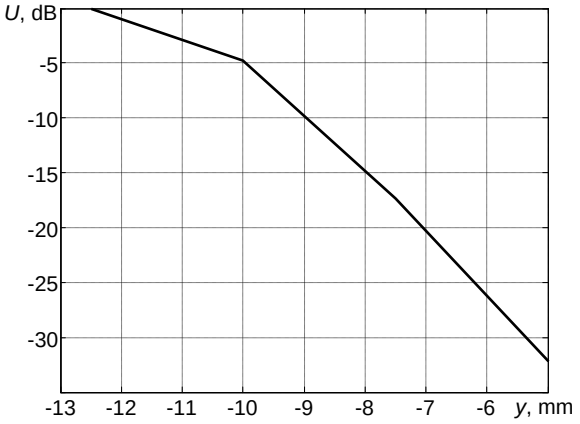

Fig.18. **Dependence of the amplitude of the reflected signals from the distance of the defect from the top surface of the rail (log scale)**

Conclusions

The presented results demonstrate the influence of the depth of the porosity defect for 35 mm weld, when the defect is located in the middle of the weld. It is necessary to say, that the results will depend on a width of the weld and a distance of the ultrasonic transducer from the edge of the weld. When the width of the weld increases and if the ultrasonic transducer array still will be positioned on the edge of the weld, the zone, where defects can be not seen, will increase as well.

Acknowledgements

The part of this work was sponsored by the European Union under the Framework-7 project “Development of an ultrasonic technique, sensors and systems for the volumetric examination of alumino-thermic rail welds” RAILECT. The Project is coordinated and managed by TWI (UK).

References

1. **Papaelias M. Ph., Roberts C., Davis C. L**. A review on non-destructive evaluation of rails: state-of the art and future development. Proc. IMechE. Vol. 222. Part F J. Rail and Rapid Transit 2008. P.367-384
2. **Ginzel E. A.** Weld inspection of ultrasonic Inspection 2. Training for non-destructive testing ultrasonic Inspection 2. Training for non-destructive testing. 1995. ISBN 1-895518-14-8
3. **Clark R.** Rail flaw detection: overview and needs for future developments. NDT&E International. 2004. Vol. 37. P.111-118.
4. Railway applications-Track Aluminothermic welding of rails. British standard BS EN 14730-1:2006.
5. Application of ultrasonic phased arrays for rail flaw inspection. U.S. Department of Transportation. Federal Railroad Administration. Washington, DC 20590. This document is available to the U.S. public through the National Technical Infromation Service Springfield, VA 22161. July 2006. DOT/FRA/ORD-06/17.
6. **Bredif P., Plu J., Pouligny P. and Poldevin C.** Phased-array method for the ut-inspection of French rail repairs. CP975. Review of Quantitative Nondestructive Evaluation. Ed by D. O.Thompson and E.Chimenti. 2008. Vol.27. American Institute of Physics 978-0-7354-0494-6/08.
7. Advances in phased array ultrasonic technology applications-Advanced practical NDT series. Chapter 1. P.5-25 http://www.olympus-ims.com/data/File/advances_book/Applications_Cha1.en.pdf
8. **Drinkwater B. W., Wilcox P. D.** Ultrasonic arrays for non-destructive evaluation: a review. NDT&E international. 2006. Vol.39. P.525-541.
9. Managing thermite weld quality for railroads. Welding Journal. January 2006. P.24-29.
10. **Fry G. T., Lawrence F. V. and Robinson A. R.** A model for fatigue defect nucleation in thermite rail welds. Fatigue Fract. Engng Mater. Struct. 1996. Vol.19. No.6. P.655-668. Printed in Great Britain.

E. Jasiūnienė, E. Žukauskas

Ultragarso bangos sąveika su poringumo defektais geležinkelio bėgio galvutėje

Reziumė

Europos geležinkelių tinkle yra keletas milijonų aliuminoterminių suvirinimo siūlių. Nors aliuminoterminio suvirinimo technologija yra gerai patikrinta, suvirinimo siūlės - kritinis geležinkelių infrastruktūros komponentas, nes jose gali atsirasti įvairių defektų. Šio darbo tikslas yra nustatyti poringumo defektų suvirinto bėgio viršutinėje dalyje (galvutėje) gylio įtaką atspindėto signalo lygiui, kai fazuota ultragarsinė gardelė yra fiksuotoje pozicijoje. Ultragarso bangos sklidimas buvo modeliuojamas naudojant baigtinių elementų paketą ANSYS ir programinės įrangos paketą CIVA. Pateikti rezultatai parodo atspindėto signalo stiprumo priklausomybę nuo defekto gylio 35 mm suvirinimo siūlėje. Kai keičiantis siūlės pločiui keitiklio atstumas nuo suvirinimo siūlės krašto išlieka tas pats, keičiasi ir zona, kurioje defektas gali būti užregistruojamas.

Pateikta spaudai 2010 03 04